



Irreversible capacities of graphite anode for lithium-ion batteries

Chunsheng Wang^{a,*}, A. John Appleby^a, Frank E. Little^b

^a Center for Electrochemical Systems and Hydrogen Research, Texas Engineering Experiment Station, Texas A&M University System, College Station, TX 77843-3402, USA

^b Center for Space Power, Texas Engineering Experiment Station, Texas A&M University, College Station, TX 77843-3118, USA

Received 26 March 2001; received in revised form 6 November 2001; accepted 6 November 2001

Abstract

Electrochemical impedance spectroscopy (EIS) and in-situ intrinsic resistance measurements were applied to sandwiched disk graphite electrodes to investigate the mechanism of formation of irreversible capacity during initial galvanostatic or potentiostatic lithium intercalation into graphite in four different electrolyte formulations. The stability of the solid | electrolyte interphase (SEI) film formed during pre-cycling eight times between 1.5 and 0.2 V versus Li | Li⁺ in 1.0 M LiPF₆ + ethylene carbonate (EC) based electrolytes was studied using EIS and in-situ intrinsic resistance measurements during subsequent cycling in the same electrolyte between 0.4 and 0.0 V, and in 1 M LiPF₆-propylene carbonate (PC) between 0.4 and 0.0 V. The purpose of the first set of results was to investigate the effect of the volume change resulting from stage transformation during Li intercalation–deintercalation on the stability of the previously formed SEI film. The second measurements were taken to study the reaction of the corresponding film in PC electrolyte. Results show that the two potential plateaus at around 0.9 and 0.6 V in the first galvanostatic charge largely correspond to solvated Li intercalation into graphite with some contribution from the formation of the SEI film. In EC-containing mixtures, this solvent has little influence on co-intercalation at 0.9 V, but can effectively inhibit the process at 0.6 V. Potentiostatic charging at 0.2 or 0.7 V accelerates co-intercalation. Although the SEI film formed during cycling in EC-containing electrolytes can inhibit PC co-intercalation during subsequent cycles in the presence of this solvent, a new layer of different SEI film may also form. © 2002 Elsevier Science B.V. All rights reserved.

Keywords: Irreversible capacity; Intrinsic resistance; Electrochemical impedance spectroscopy; Li-ion batteries

1. Introduction

The electrolytes used for lithium-ion cells are thermodynamically unstable at potentials close to the Li | Li⁺ electrode potential, and solvents such as propylene carbonate (PC) can co-intercalate with Li into graphite with subsequent reduction and/or decomposition of solvent. It has been suggested that this is because of the formation of solvent lithium/graphite compounds of Li(sol)_yC₆ type (graphite insertion compounds, GICs) may be more favorable than the formation of LiC₆ during insertion [1]. Fortunately the decomposition products of some electrolyte solvents, e.g. ethylene carbonate (EC) form a stable solid | electrolyte interphase (SEI) film on the graphite surface, which is permeable

to Li⁺ cations, but is electronically insulating, and prevents further electrolyte decomposition and co-insertion during cycling. The success of rechargeable lithium-ion batteries is largely due to the stable formation of such SEI films on graphite or carbon anodes. The stability of the SEI film determines the safety, power capability, self-discharge rate, and cycle life of the battery.

SEI film formation on a graphite surface and solvated lithium intercalation between the graphite layers in the first few Li intercalation–deintercalation cycles are accompanied by irreversible consumption of lithium and electrolyte. Since the cathode is the only source of lithium in a lithium-ion battery, these losses are detrimental to specific energy and must be minimized for optimum performance. The irreversible capacity associated with the use of graphite is extremely dependent on electrolyte composition, the rate of lithiation during the formation cycles, temperature, the surface structure of graphite, and the extent of charge–discharge cycles [2].

* Corresponding author. Tel.: +1-979-845-2033; fax: +1-979-845-9287.

E-mail address: cswang@tamu.edu (C. Wang).

PC and EC are the most commonly used high permittivity solvents for lithium-ion batteries. It is well known that EC-based electrolytes are always used with graphite anodes. In contrast, PC-based electrolytes are used with carbons, and are not compatible with graphite anodes due to both continuous PC decomposition without stable passive graphite|electrolyte interphase formation, and continuous PC–Li co-intercalation into the graphite planes [3]. Nevertheless, PC is still an attractive electrolyte, especially for low-temperature operation, because of its high salt solubility and low melting point ($-55\text{ }^{\circ}\text{C}$).

One approach to suppressing irreversible solvated lithium intercalation is by first precycling a graphite electrode once in an EC- or dimethyl carbonate (DMC) based electrolyte, then recycling it in a PC-based electrolyte [4,5]. It is believed that a stable passivating SEI film formed in EC- or DMC-based electrolyte may retard co-intercalation of PC during subsequent cycling, but any changes in the SEI film after cycling in PC-based electrolytes are still unclear. A low irreversible capacity requires that the thin SEI film should have good adhesion to graphite, high mechanical strength, and high flexibility to accommodate the volume change during intercalation–deintercalation. As far we know, no work on these topics has been reported.

In this paper, the irreversible capacity associated with solvated Li intercalation and SEI formation on JM 287 (Johnson Matthey, Inc.) graphite [6] during the first few galvanostatic and potentiostatic cycles in different electrolytes has been investigated using electrochemical impedance spectroscopy (EIS) along with in-situ intrinsic resistance measurement. The changes in the SEI film in PC-based electrolytes after eight previous cycles in EC + PC + DMC (1:1:3) electrolyte were also studied. The influence of volume change due to stage transformation on the stability of SEI film was monitored by changes in the irreversible capacity on cycling between 0.4 and 0.0 V versus Li|Li⁺ after eight cycles between 1.5 and 0.2 V.

2. Experimental

2.1. Electrode and cell preparation

Electrodes consisting of ca. 50 mg of ball-milled JM 287 graphite powder (particle size ca. 15 microns, BET area as received $13.5\text{ m}^2\text{ g}^{-1}$, after milling $>30\text{ m}^2\text{ g}^{-1}$)¹ between two nickel screens (geometric area 2.0 cm^2) were prepared as in our previous work [6–10]. The electrochemical measurements were conducted in a three-electrode PTFE cell containing two lithium foils

¹ The material was identical to that used previously [6], but earlier papers neglected to state that it was further milled.

as both counter and reference electrodes (REs). All potentials given are versus the Li|Li⁺ RE in the four electrolytes studied, which were 1.0 M LiPF₆ in 1:1 (by volume) E + DMC, 1:1:3 EC + PC + DMC, 4:1:3:2 EC + PC + DMC + EMC, and pure PC. All were High Purity Lithium Battery Grade (Mitsubishi Chemical Company). Charge (lithium intercalation) and discharge (lithium deintercalation) characteristics were measured using an Arbin (College Station, TX) automatic battery cycler. In-situ intrinsic resistances were measured by the application of a 10 mA constant current across the electrode. The electrodes were charged–discharged on one side only, and the voltage differences across both sides were used to measure their overall intrinsic resistances. This refers to those physical elements present within the thickness of the electrode, including the electronic resistance of the series-parallel array of graphite particles themselves, the electronic contacts with and within the binder and ionic (electrolytic) contacts, and the electronic resistances of the current collectors and the contact resistances between them and the neighboring graphite particles. This intrinsic resistance and transmissive impedance can be evaluated by the voltage across the electrode with flowing d.c. current and by transmissive EIS methods, respectively.

Potentiostatic charge–discharge was applied on the electrodes in the range 3.0–0.2 V using different programmed potential steps, viz., from 3.0 to 0.7 to 0.2 V, then back to 0.7 and to 3.0 V, and second, between 1.5 and 0.2 V. Each step was initiated only when the current became less than 1.0 μA . Galvanostatic charge–discharge was also used between 1.5 and 0.2 V. After eight potentiostatic or galvanostatic charge–discharge cycles to form the SEI film completely, some electrodes were again cycled in the same electrolyte between 0.4 and 0.0 V to investigate the influence of volume change of the graphite electrode on SEI film stability. Other electrodes which had been pre-cycled eight times between 1.5 and 0.2 V in the EC + PC + DMC (1:1:3) and EC + PC + DMC + EMC (4:1:3:2) electrolytes were transferred to the PC electrolyte at 1.5 V. After a 20 h rest period, they were then cycled galvanostatically between 0.4 and 0.0 V in the PC electrolyte.

2.2. EIS measurement

The EIS was measured over the frequency range 65 kHz–1.0 mHz at a potentiostatic signal amplitude of 5 mV, using Solatron equipment as in previous work [6–10]. In all cases, EIS measurements were performed after a rest period of 3 h. For transmissive impedance measurement, EIS measurements were taken between the two sides of the electrode, connecting the RE₂ and WE terminals of the Solatron interface together to one of the sides, and RE₁ and CE to the other (Fig. 1). For

electrochemical reaction kinetics measurements, EIS scans were made by connecting the terminals RE₂ plus WE terminals of the Solatron interface to both sides of the graphite working electrode (WE). A schematic diagram of the cell and the different interface terminal-to-electrode connections, including the geometrical arrangement of the counter and REs for each protocol, is shown in Fig. 1. The physical meaning of the two EIS measurement protocols have been discussed in our previous papers [8].

3. Results and discussion

3.1. Initial galvanostatic and potentiostic charge–discharge behavior of anodes between 1.5 and 0.2 V (single phase region)

To remove the influence of electrode volume changes resulting from stage transformations during Li intercalation–deintercalation, fresh electrodes were first cycled in each of the electrolytes. In 1 M LiPF₆ + PC, the 10 mA d.c. current passed through the electrode for intrinsic resistance measurement was interrupted because

graphite exfoliation due to PC intercalation results in a significant voltage across the electrode. The potential on both side of the electrode was, therefore, monitored instead in this case. The first galvanostatic charge–discharge curves of JM 287 electrodes in the four electrolytes are shown in Fig. 2.

The potential profiles in three EC-based electrolytes show two similar potential plateaus at around 0.9 and 0.6 V, while only one potential plateau around 1.0 V appeared in PC. Winter et al. [1,11,12] believe that both potential plateaus at 0.9 and 0.6 V mainly result from the progressive staging of solvated Graphite Intercalation Compounds (GIC), with some contribution from SEI film formation [3]. For the electrode in PC electrolyte, the potential at the side being charged began to decrease at around 300 mA h g⁻¹ capacity, and dropped more rapidly at 550 mA h g⁻¹, while the potential at the opposite side was stable at about 1.0 V during the entire charge period. This suggests that exfoliation by PC intercalation fractured the electrode, in agreement with the results of Aurbach et al. [13] and Yoshio et al. [14] Adding a small amount of EC (20%) to the PC + DMC electrolyte significantly suppressed the PC intercalation capacity loss at around 1–0.9 V

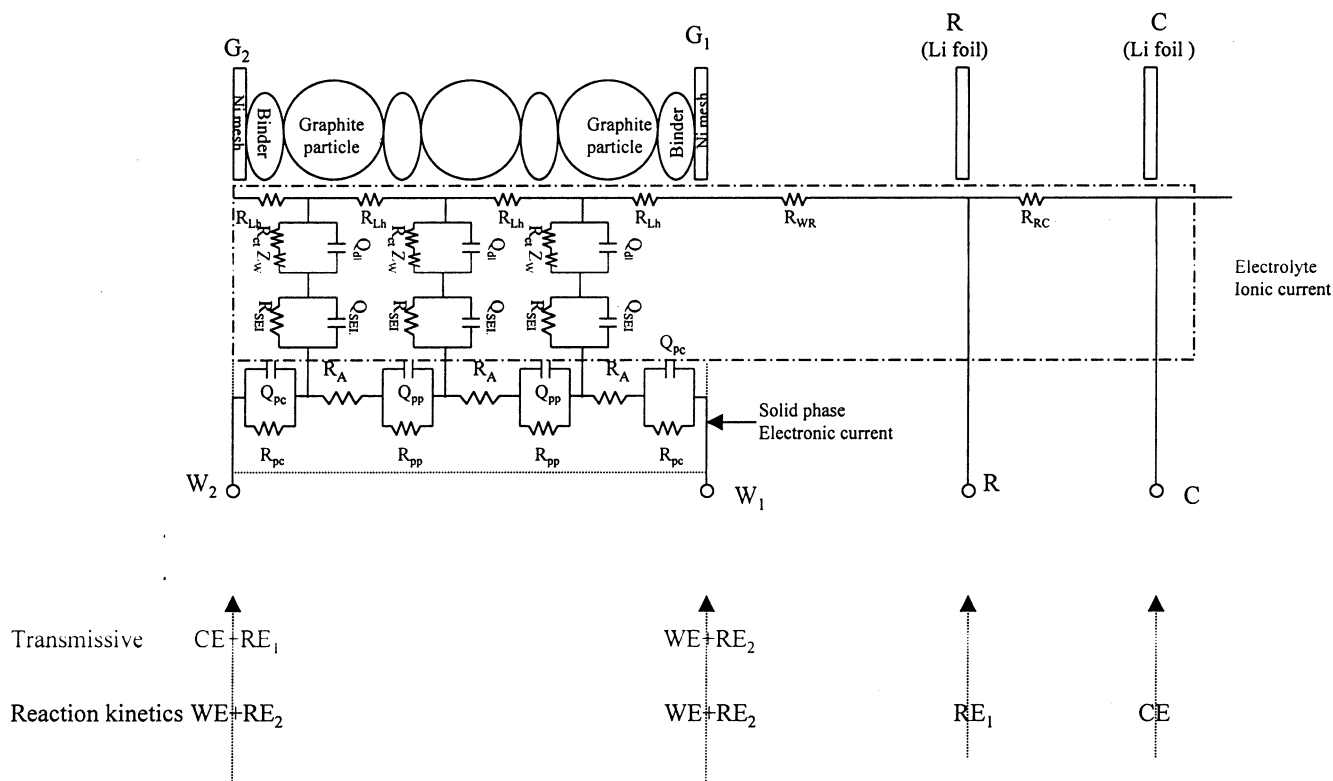


Fig. 1. Schematic diagram of cell with porous ion insertion anode and special Solatron electrochemical interface terminal-to-electrode connections. The transmission line equivalent is also shown. R_G , R_{Lh} , R_{WR} , and R_{RC} : electronic resistance of graphite particle, ion resistance of electrolytes in the pores, reference electrode (RE) to working electrode (WE) ionic resistance, and RE to counter electrode (CE) ionic resistance. R_{pc} , R_{pp} , R_{SEI} and R_{ct} : Graphite particle-to-current collector, particle-to-particle, SEI film and charge-transfer resistances. Q_{pc} , Q_{pp} , Q_{SEI} , and Q_{d1} : Constant-phase elements for particle-to-current collector, for particle-to-particle, for the SEI film and for the double-layer, respectively. Z_w : Finite Warburg element for lithium diffusion in graphite.

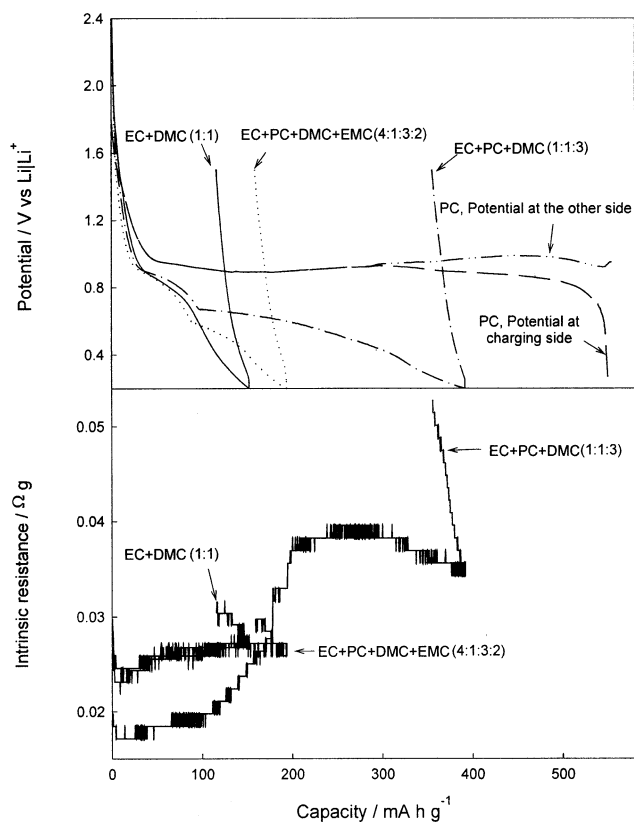


Fig. 2. Initial charge–discharge potential and intrinsic resistance profiles for JM 287 graphite in the potential range between 1.5 and 0.2 V. Charge–discharge current: 7 mA g^{-1} . Current for measuring intrinsic resistance: 10 mA . For JM 287 graphite in $1 \text{ M LiPF}_6 + \text{PC}$ electrolyte, only the voltage across the graphite electrode (without d.c. current) was monitored due to the high contact resistance induced by graphite exfoliation.

from 520 to 60 mA h g^{-1} . However, further increasing the EC content to 40% in PC + DMC + EMC electrolyte decreased intercalation only between 0.6 and 0.2 V, and had little influence on the irreversible capacity at 0.9 V. The reason for this may be explained by the fact that both EC and DMC intercalate into graphite at 0.9 V [12]. The passivating SEI film formed from EC decomposition products gives complex three-dimen-

sional solvated ternary GICs, which can inhibit the solvent intercalation at 0.6 V. Similar behavior was reported by Yu et al. [15] for KS 10 graphite during the first charge–discharge cycle in the EC + PC + DMC (1:1:3) and EC + DME (1:1) electrolytes. The irreversible capacities increased with decreasing the EC content of the electrolytes in the order EC + DMC (EC 50 vol.%) < EC + PC + DMC + EMC (EC 40%) < EC + PC + DMC (EC 20%) < PC although the electrode deintercalation capacities were similar in the three EC-based electrolytes.

The reduction products of the solvent, whether formed as an SEI surface film or intercalated into the graphite planes, are electronic resistors. Therefore, measurements of intrinsic resistance may be used to monitor the formation of SEI films and GICs, as Fig. 2 shows. As expected, the intrinsic resistance of JM 287 graphite in EC + PC + DMC (20% EC) showed two increasing steps at potentials around 0.9 and 0.6 V. The much higher increase at 0.6 than at 0.9 V is probably due to the larger amount of solvent intercalation into graphite at 0.6 V, which results in higher irreversible capacities. The second increase in intrinsic impedance at about 0.6 V disappeared as the electrolyte EC content was increased. Therefore, both the potential profiles and intrinsic resistance measurements suggest that EC decomposition compounds on the external surfaces of JM 287 form an effective protective film, which suppresses solvent intercalation. The decrease in intrinsic resistance from the open-circuit potential to 0.9 V corresponds to increasing conductivity of the graphite host material [16].

The passivating SEI film formed by EC decomposition not only inhibits further solvent intercalation into the graphite planes at 0.6 V, but also slows reaction kinetics for lithium intercalation–deintercalation, as is evident from kinetic EIS measurements taken during initial charging to 0.2 V (Fig. 3). The impedance of the SEI film, obtained from the first relaxation loop, decreases in the order EC + DMC (EC 50%) > EC + PC + DMC + EMC (EC 40%) > EC + PC + DMC (EC 20%), which is in the reverse order of the irreversible

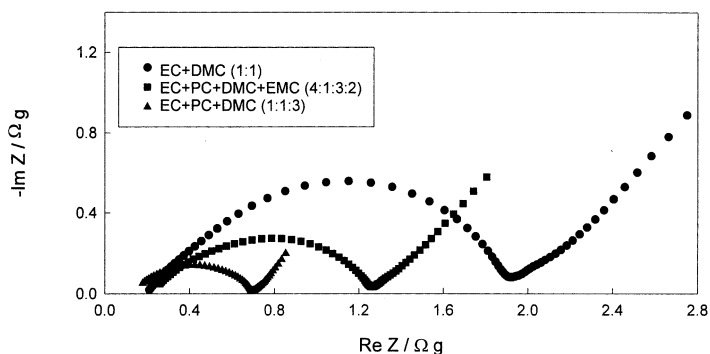


Fig. 3. Nyquist plots of reaction kinetics for initial lithium intercalation into JM 287 graphite to 0.2 V in different electrolytes.

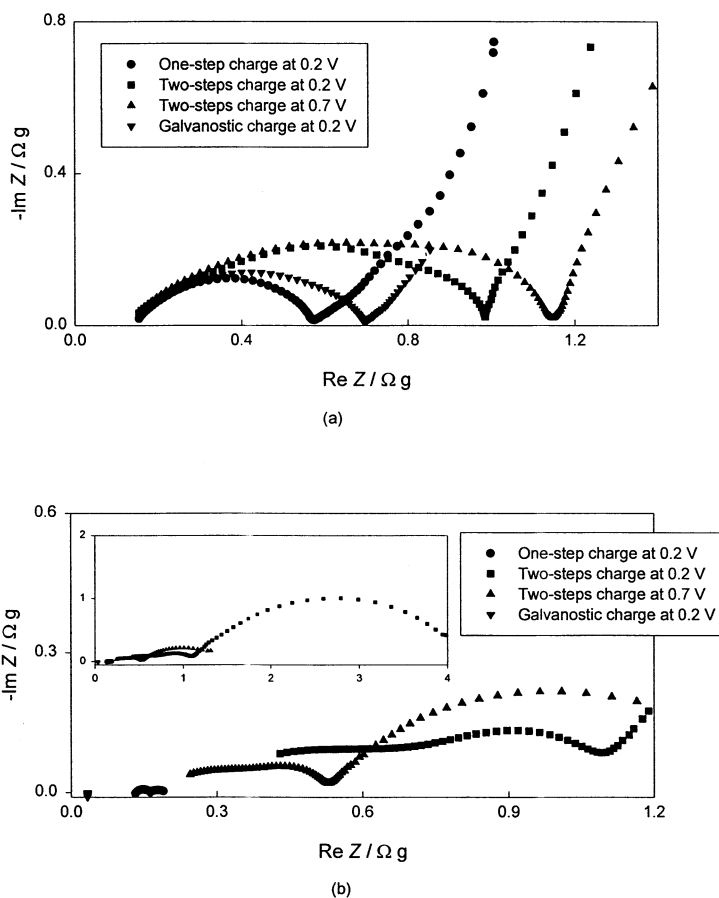


Fig. 4. Nyquist plots of reaction (a) and transmissive impedances (b) for Li potentiostatic intercalation into JM 287 graphite in EC + PC + DMC using one- and two-steps charge methods. The reaction and transmissive impedances of a JM 287 graphite electrode charged using the galvanostatic method is also shown in Fig. 6 for comparison.

capacities. The transmissive impedance shows a pure electronic resistance with a value similar to those measured using a 10 mA d.c. current (Fig. 2). No semicircles related to the graphite particles-to-particles and particles-to-current collector are observed in transmissive impedance, which suggested that solvated Li intercalation into graphite increases only the electronic resistance of the electrode particles, and the SEI film mostly forms on the external surface exposed to electrolyte, not between the particles themselves and in the particle to current collector junction.

The initial galvanostatic charge–discharge behavior of JM 287 graphite in the three EC-containing electrolytes may be reasonably explained by the Winter's mechanism that both potential plateaus at 0.9 and 0.6 V result from the successive stages of solvent GIC. However, Yu et al. [15] and Aurbach et al. [17] believe that only the potential plateau at 0.6 V results from solvent co-intercalation, and they attribute the 0.9 V plateau to SEI formation. If this is correct, potentiostatic charging for a long period below 0.9 V, but above the second potential plateau at 0.6 V, may create an effectively passivating SEI film to prevent subsequent

solvent co-intercalation at the second potential plateau. Moreover, if the graphite electrode is potentiostatically charged from its initial open-circuit potential to a low potential value above 0.2 V, to avoid the influence of volume change due to the stage transformation, then SEI formation and solvent co-intercalation will compete with each other. If electrolyte decomposition on the graphite surface is more rapid than solvent co-intercalation at this overpotential so a passivating film can form, solvent co-intercalation may be more effectively prevented than when galvanostatic charging is used.

To test this approach, potentiostatic charge–discharge was applied on two identical electrodes between 3.0 and 0.2 V using two differently programmed potential steps. These were from 3.0 to 0.7 to 0.2 V, and then back to 0.7 V, followed by 1.5 V (called two-step charge–discharge), and from 3.0 to 0.2 V, and then back to 1.5 V (one-step charge–discharge). Each step was initiated only when the current became less than 1.0 μA . At the end of each charge step, EIS scans were performed to compare the kinetic and transmissive impedances of the two electrodes following a 3 h rest period. Fig. 4 shows the corresponding Nyquist plots

obtained in EC + PC + DMC. The kinetic and transmissive impedances for the galvanostatic intercalation of Li in the same electrolyte are also shown in Fig. 4 for comparison. The results shown may be summarized as follows.

1. The electrode charged using one-step potentiostatic charging had a higher transmissive resistance but a lower kinetic resistance than when galvanostatically charged. The two depressed semicircles in the transmissive impedance EIS, which are attributed to particle-to-particle and particle-to-current contact impedance, [7–9] may result from graphite exfoliation via decomposition of a large amount of solvent co-intercalated at 0.2 V. Solvent co-intercalation increases the electronic resistances of the graphite particles, as is shown by the high value of the intersection point of the high frequency line with the real axis (Fig. 4b). Reduction of electrolyte on the graphite surface, accompanied by decomposition of intercalated solvated material and graphite exfoliation, forms a porous, less passivating SEI film, as is evident from the low kinetic impedance in Fig. 4a. Therefore, impedances in Fig. 4 suggested that the reaction rate due to solvent co-intercalation into

graphite is faster than the rate of SEI film formation under potentiostatic pulse charge conditions from open-circuit to 0.2 V in EC + PC + DMC.

2. Two-step potential pulse charging at 0.7 V resulted in more serious solvent co-intercalation and exfoliation, giving an even higher transmissive impedance and kinetic impedance, as is shown in Fig. 4. Thus, the potential plateau at around 0.9 V may most likely be associated with solvent co-intercalation, and not to SEI film formation. Upon further potential pulse charging from 0.7 to 0.2 V, i.e. below the second solvent co-intercalation plateau at 0.6 V, additional solvent co-intercalates, which results in further exfoliation. This is evident from an increase in transmissive impedance from 1.2 to 4 Ω g, and supports the conclusion that the SEI film formed by potential pulse charging at 0.7 V is less passivating, allowing solvent co-intercalation at 0.6 V.

3.2. Galvanostatic charge–discharge behavior of anodes between 0.4 and 0 V (stage transformation region) after eight galvanostatic or potentiostatic charge–discharge cycles between 1.5 and 0.2 V

After eight galvanostatic charge–discharge cycles to allow attainment of their fully reversible capacities, the electrodes used in Fig. 2 were further galvanostatically charged to 0.0 V. After resting at open circuit for 3.0 h, the electrodes were discharged to 0.4 V. Fig. 5 shows their potential and intrinsic resistance profiles between 0.4 and 0.0 V after eight galvanostatic charge–discharge cycles in the three EC-based electrolytes. Although the deintercalation capacities in the three electrolytes were similar (approximately 200 mA h g⁻¹), the irreversible capacity in EC + PC + DMC was much larger (330 mA h g⁻¹) than those in the other two electrolytes (around 90 mA h g⁻¹). Hence, the mechanical strength and flexibility of the SEI film formed during eight galvanostatic charge–discharge cycles between 1.5 and 0.2 V is not great enough to accommodate the graphite volume change on stage transformation. This is especially so for the SEI film formed in EC + PC + DMC. It would appear that the irreversible capacities mainly result from growth of further SEI film rather than from solvated Li co-intercalation, because no increase in the intrinsic resistance due to solvent intercalation appearing in this potential range even in EC + PC + DMC (Fig. 5), even though the SEI film impedance increased in the potential range 0.2–0.08 V (Fig. 6). This additional SEI film growth may occur in cracks in the electrode which result from swelling of the graphite particles. Fig. 6 shows the kinetic impedances at 0.2 and 0.08 V after 8 galvanostatic charge–discharge cycles between 1.5 and 0.2 V in EC + PC + DMC.

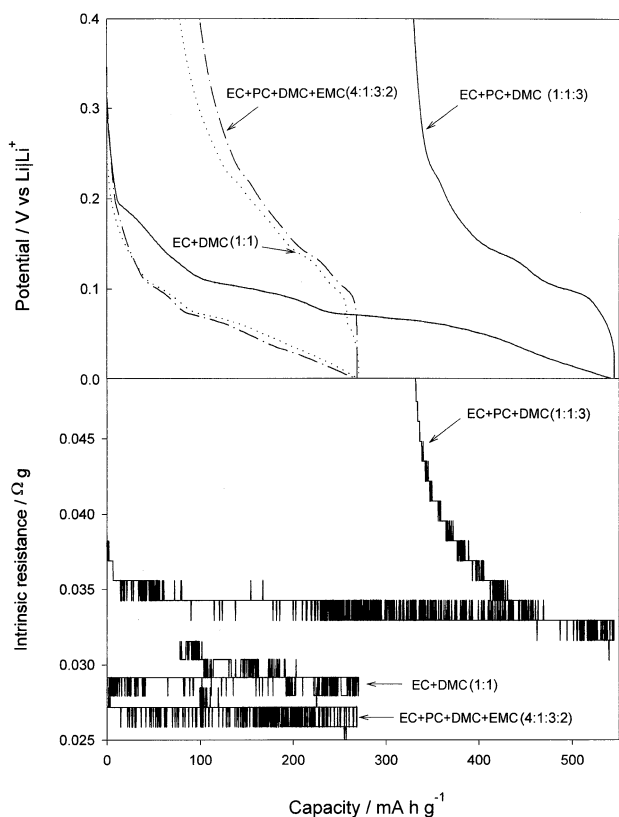


Fig. 5. Initial charge–discharge potential and intrinsic resistance profiles for JM 287 graphite in the potential range between 0.4 and 0 V after eight galvanostatic charge–discharge cycles in EC + PC + DMC and EC + PC + DMC + EMC electrolytes. Charge–discharge current: 7 mA g⁻¹, current for measuring intrinsic resistance: 10 mA.

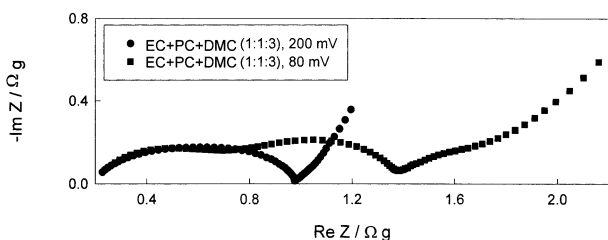


Fig. 6. Nyquist plots of reaction kinetics impedance of JM 287 graphite electrode after eight galvanostatic charge–discharge cycles between 1.5 and 0.2 V, in EC + PC + DMC electrolyte.

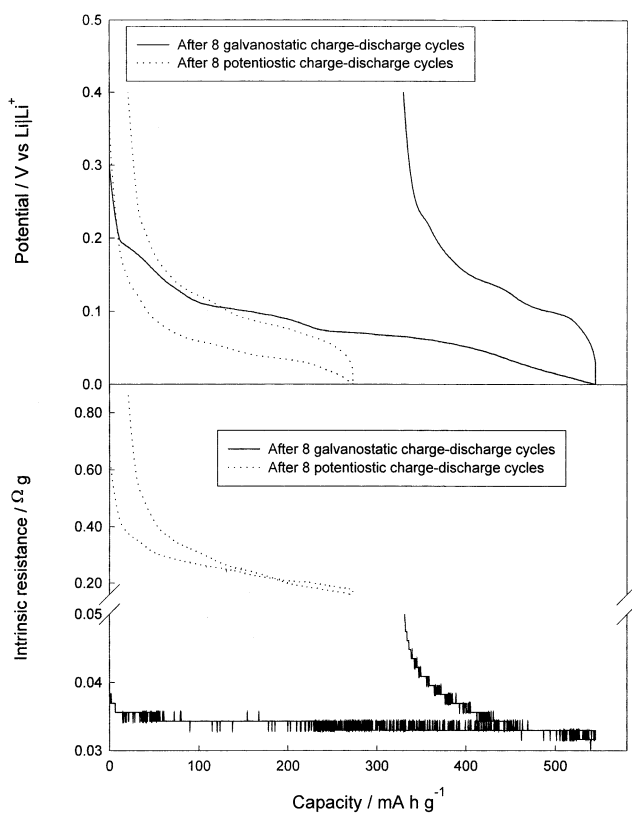


Fig. 7. Initial charge–discharge potential and intrinsic resistance profiles for JM 287 graphite in the potential range between 0.4 and 0 V after eight potentiostatic charge–discharge cycles between 1.5 and 0.2 V in EC + PC + DMC electrolyte. Charge–discharge current: 7 mA g^{-1} , current for measuring intrinsic resistance: 10 mA .

The SEI film formed in EC + PC + DMC + EMC and EC + DMC may be considered as passivating (i.e. of barrier type), because it inhibits solvent intercalation at 0.6 V (Fig. 2). Moreover, the small increase in irreversible capacity on further cycling between 0.4 and 0 V (Fig. 5) suggests that the passivating film formed in EC + PC + DMC + EMC and EC + DMC is more effective than that formed in EC + PC + DMC in not only suppressing solvent intercalation into graphite, but also in accommodating the volume change due to stage transformation.

Unlike preliminary galvanostatic charge–discharge cycling, preliminary one-step potentiostatic charge–discharge cycling carried out eight times in EC + PC + DMC electrolyte assists in producing a more passivating SEI film which better accommodates the volume change in the stage transformation region (Fig. 7). At the same time, more solvent co-intercalates, resulting in exfoliation and a high transmissive impedance (Fig. 4b). However, the different methods of preliminary cycling between 1.5 and 0.2 V have little influence on performance between 0.4 and 0.0 V in EC + PC + DMC + EMC electrolyte, as Fig. 8 shows. Hence, both methods of pretreatment only affect the cycling performance of electrodes carrying a porous SEI film.

3.3. SEI film stability after transfer from EC + PC + DMC (1:1:3) to PC electrolyte

After eight galvanostatic charge–discharge cycles between 1.5 and 0.2 V in EC + PC + DMC electrolyte, an electrode was transferred to PC electrolyte at 1.5 V. The potential and intrinsic resistance profiles of the eighth charge–discharge cycle in EC + PC + DMC, followed by the changes during a 20 h rest period, and subsequent cycles in PC electrolyte are shown in Fig. 9.

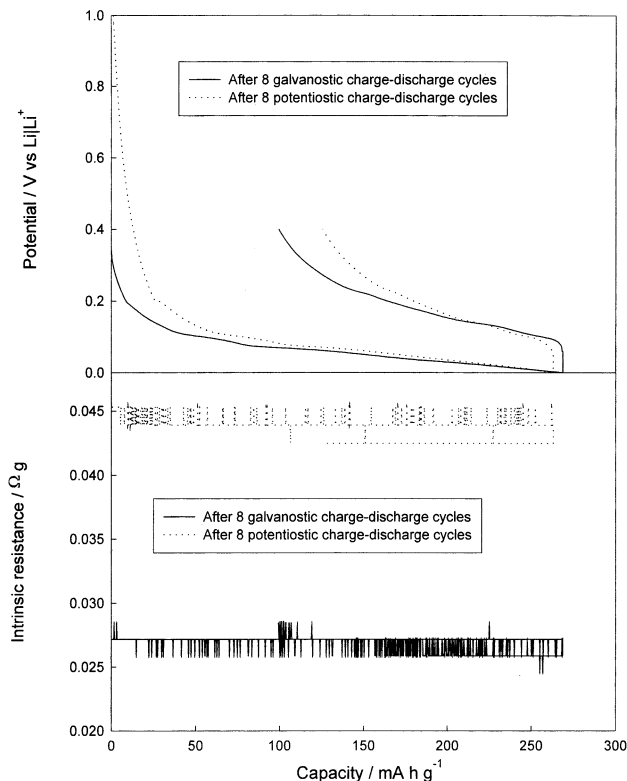


Fig. 8. Initial charge–discharge potential and intrinsic resistance profiles for JM 287 graphite in the potential range between 0.4 and 0 V after eight potentiostatic charge–discharge cycles between 1.5 and 0.2 V in EC + PC + DMC + EMC electrolyte. Charge–discharge current: 7 mA g^{-1} , current for measuring intrinsic resistance: 10 mA .

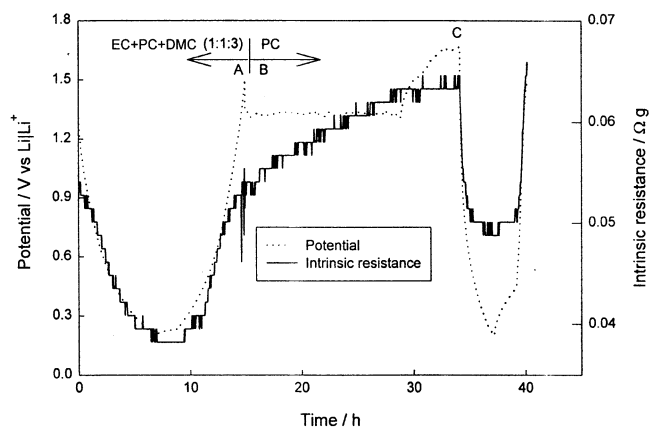


Fig. 9. Potential and intrinsic resistances of JM 287 graphite during the eighth charge–discharge cycle in EC-PC-DMC electrolyte, a rest for 20 h in PC and charge–discharge in PC. At 1.5 V in EC + PC + DMC electrolyte (A point), after transfer to PC electrolyte (B point), and rest for 20 h in PC electrolyte (C point), EIS is performed to measure the reaction impedance and intrinsic impedance. Charge–discharge current: 5.8 mA g^{-1} , current for measuring intrinsic resistance: 10 mA.

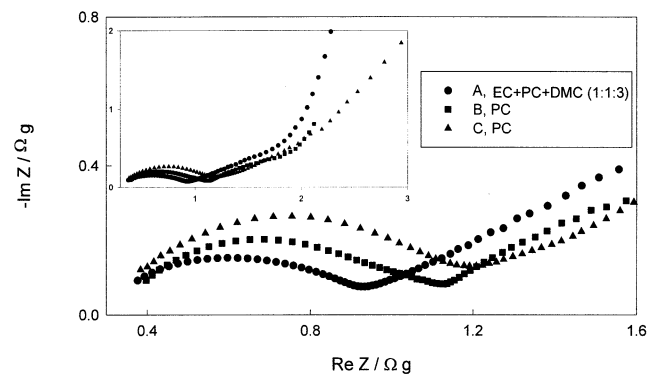


Fig. 10. Nyquist plots for reaction kinetics impedances at the points specified in Fig. 9 using Protocols D and A, respectively.

The electrode was allowed to rest for 3 h between each charge and discharge. The EIS was performed at different rest times, marked A, B, C in Fig. 9. The potential profile in Fig. 9 shows that JM 287 graphite is almost reversible on the eighth charge–discharge cycle in EC + PC + DMC electrolyte. After transfer to PC, the electrode potential was stable during the first 15 h of rest time, and then began to increase, reaching 1.62 V at 20 h. No potential plateaus at around 0.9 and 0.6 V appeared following Li intercalation in PC using the same charge–discharge current, which indicates that the SEI film formed during pre-cycling in EC + PC + DMC can inhibit PC co-intercalation. This result is in agreement with previously reported work [5]. However, careful comparison of the charge–discharge potential profile of the electrode in PC and in EC + PC + DMC shows that the capacity in the first electrolyte is less than that in the second. The low capacity in PC electrolyte is due to slower reaction kinetics, since the

potential recovery during the 3.0 h of rest time after charging to 0.2 V is larger in PC than in EC + PC + DMC. The slow reaction kinetics in PC electrolyte may be largely attributed to increased SEI film impedance, as is shown by the increase in size of the first Nyquist plot semicircle as a function of rest time in PC (Fig. 10). Therefore, it is possible that after transfer of the electrode to the new electrolyte, PC reacted with the previously-formed SEI film during the rest period, producing a further layer which increased the kinetic impedance (Fig. 10), at the same time inhibiting PC intercalation following cycling in this electrolyte. That the newly-formed SEI film grows further during the following charge–discharge in PC is evident from the large increase in the size of the first Nyquist semicircle (Fig. 11).

4. Conclusion

JM 287 (Johnson Matthey, Inc.) graphite powder disks sandwiched between two nickel screens were used as WE in 1.0 M lithium hexafluorophosphate in mixed carbonate ester electrolytes. The formation of a SEI film and the co-intercalation of solvated Li during initial galvanostatic and potentiostatic Li intercalation in four types of electrolyte were investigated using EIS and in-situ intrinsic resistance measurements. The stability of the SEI film in the graphite stage transformation region before and after transferring from EC-based electrolytes to PC solution was also studied by EIS and intrinsic resistance measurement. The potential profiles for initial galvanostatic Li intercalation in EC-based electrolytes show two similar potential plateaus at

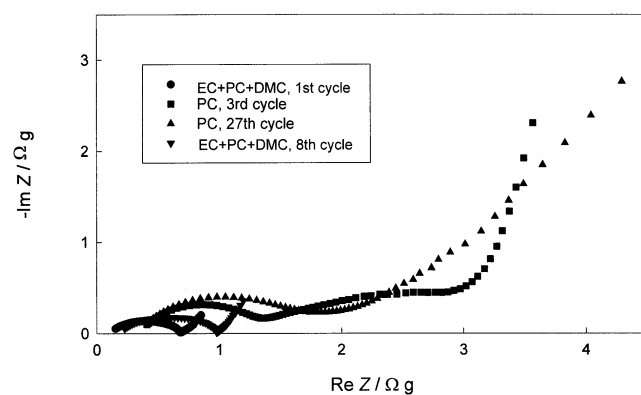


Fig. 11. Nyquist plots for kinetics of lithium intercalation–deintercalation impedance for JM 287 graphite pretreated in EC + PC + DMC electrolyte for eight cycles and transferred to PC for 27 cycles. The EIS scans are measured at 0.2 V. After eight cycles in EC + PC + DMC electrolyte between 1.5 and 0.2 V, the electrode is transferred to PC electrolyte, and further charge–discharged in PC electrolyte between 1.5 and 0.2 V for another three cycles using the same charge–discharge current. After that the electrode is cycled in PC electrolyte between 0.4 and 0 V for 27 cycles.

around 0.9 and 0.6 V, respectively. These may largely be attributed to solvated Li co-intercalation into graphite, with some contribution from the formation of the SEI film on the electrode surface. A porous, less passivating SEI film is formed by the decomposition of electrolytes with high PC content (for example EC + PC + DMC, 1:1:3), which allows more solvent to intercalate into graphite during galvanostatic charging. This phenomenon becomes more marked when the electrode is potentiostatically charged at 0.2 or 0.7 V. The volume change due to Li_xC_6 stage transformation disturbs the previously-formed SEI film, especially if it is porous, which induces additional irreversible capacity. The SEI film formed on the electrode surface during pre-cycling in EC-based electrolyte can inhibit solvent co-intercalation during subsequent cycling in PC electrolyte. However, a new layer of SEI film may then form on the original SEI surface, resulting in an increase in the kinetic Li intercalation–deintercalation impedance during further cycling in this electrolyte.

References

- [1] M. Winter, P. Novak, A. Monnier, *J. Electrochem. Soc.* 145 (1998) 428.
- [2] M.C. Smart, B.V. Ratnkumar, S. Surampudi, Y. Wang, X. Zhang, S.G. Greenbaum, A. Hightower, C.C. Ahn, B. Fultz, *J. Electrochem. Soc.* 146 (1999) 3963.
- [3] G.C. Chung, H.J. Kim, S.I. Yu, S.H. Jun, J.W. Choi, M.H. kim, *J. Electrochem. Soc.* 147 (2000) 4391.
- [4] D. Billaud, A. Naji, P. Willmann, *J. Chem. Soc., Chem. Commun.* 1867 (1995).
- [5] A. Naji, J. Ghanbaja, P. Willmann, D. Billaud, *Carbon* 35 (1997) 845.
- [6] C. Wang, I. Kakwan, A.J. Appleby, F.E. Little, *J. Electroanal. Chem.* 489 (2000) 55.
- [7] C. Wang, A.J. Appleby, F.E. Little, *J. Electroanal. Chem.* 497 (2001) 33.
- [8] C. Wang, A.J. Appleby, F.E. Little, *Electrochim. Acta* 46 (2001) 1793.
- [9] C. Wang, A.J. Appleby, F.E. Little, *J. Power Sources* 93 (2001) 175.
- [10] C. Wang, A.F. Rakotondrainibe, A.J. Appleby, F.E. Little, *J. Electrochem. Soc.* 147 (2000) 4432.
- [11] M. Winter, G.H. Wrodnigg, J.O. Besenhard, W. Biberacher, P. Novak, *J. Electrochem. Soc.* 147 (2000) 2427.
- [12] J.O. Besenhard, M. Winter, J. Yang, W. Biberacher, *J. Power Sources* 54 (1995) 228.
- [13] D. Aurbach, Y. Ein-Eli, O. Chusid, Y. Carmeli, M. Babai, H. Yamin, *J. Electrochem. Soc.* 141 (1994) 603.
- [14] M. Yoshio, H. Wang, K. Fukuda, Y. Hara, Y. Adachi, *J. Electrochem. Soc.* 147 (2000) 1245.
- [15] P. Yu, J.A. Ritter, R.E. White, B.N. Popov, *J. Electrochem. Soc.* 147 (2000) 1280.
- [16] M.S. Dresselhaus, G. Dresselhaus, *Adv. Phys.* 30 (1981) 139.
- [17] D. Aurbach, M.D. Levi, A. Schechter, *J. Phys. Chem. B* 101 (1997) 2195.